Physics and Imaging in Radiation Oncology 34 (2025) 100755

Contents lists available at ScienceDirect

Physics and Imaging in Radiation Oncology

journal homepage: www.sciencedirect.com/journal/physics-and-imaging-in-radiation-oncology

Original Research Article

# Partial adaptation for online-adaptive proton therapy triggered by during-delivery treatment verification: Feasibility study on prostate cancer treatments☆

Virginia Gambetta[a,b,1,*], Victoria Pieta[a,1,3], Jonathan Berthold[a,c,d], Tobias Hölscher[a,e], Albin Fredriksson[f], Christian Richter[a,b,e,g,2], Kristin Stützer[a,b,2]

[a] OncoRay – National Center for Radiation Research in Oncology, Faculty of Medicine and University Hospital Carl Gustav Carus, TUD Dresden University of Technology, Helmholtz-Zentrum Dresden-Rossendorf, Fetscherstr. 74, PF 41, 01307 Dresden, Germany
[b] Helmholtz-Zentrum Dresden-Rossendorf, Institute of Radiooncology – OncoRay, Bautzner Landstr. 400, 01328 Dresden, Germany
[c] CASUS – Center for Advanced Systems Understanding, Helmholtz-Zentrum Dresden-Rossendorf, Untermarkt 20, 02826 Görlitz, Germany
[d] Helmholtz-Zentrum Dresden-Rossendorf, CASUS - Center for Advanced Systems Understanding, Bautzner Landstr. 400, 01328 Dresden, Germany
[e] Department of Radiotherapy and Radiation Oncology, Faculty of Medicine and University Hospital Carl Gustav Carus, TUD Dresden University of Technology, Fetscherstr. 74, PF 50, 01307 Dresden, Germany
[f] RaySearch Laboratories AB, Box 45169, SE-104 30 Stockholm, Sweden
[g] German Cancer Consortium (DKTK), Partner Site Dresden, and German Cancer Research Center (DKFZ), Im Neuenheimer Feld 280, 69192 Heidelberg, Germany

ARTICLE INFO

*Keywords:*
Online-adaptive proton therapy
Treatment verification
Prompt gamma imaging
Partial adaptation
Verification-triggered online adaptation
Prostate cancer

ABSTRACT

*Background and Purpose:* Online treatment verification during proton therapy delivery may detect deviations due to anatomical changes occurring along the treatment course and trigger immediate intervention, if necessary. We investigated the potential of partial plan adaptation in two-field prostate cancer treatments as a solution for online-adaptive proton therapy (OAPT) after the detection of relevant treatment deviations during the first field delivery.

*Materials and Methods:* In a retrospective study, ten fractions from eight prostate cancer patients with prompt gamma imaging (PGI) detected treatment deviations, which were confirmed on respective in-room control computed tomography (cCT) scans, were considered. For each cCT, a dose-mimicking-based robust partial adaptation reoptimized the second field by considering the suboptimal dose delivery of the first non-adapted, PGI-monitored field. The results were compared to the non-adapted scenario and upfront full adaptation (both fields) in terms of achievable target coverage (prescription: 48 Gy/60 Gy to low-risk/high-risk target) and organ-at-risk (OAR) sparing.

*Results:* Partially adapted plans showed comparable target coverage (median $D_{98\%}$: 99.9%/98.0% for low-/high-risk target) to fully adapted plans (100.3%/98.7%) and were superior to non-adapted plans (98.7%/94.5%). Achievable OAR sparing was patient-specific depending on the proximity to the target region, but within clinical goals for the partially and fully adapted plans.

*Conclusions:* Partial adaptation triggered mid-delivery of a fraction can still generate plans of comparable conformity to full adaptation, even in the case of plans with only two, opposing fields. A verification-triggered OAPT may therefore become an alternative to upfront OAPT, saving time and imaging dose in fractions without relevant anatomy changes.

☆ This article is part of a special issue entitled: 'Physics highlights from ESTRO 2024' published in Physics and Imaging in Radiation Oncology.

* Corresponding author at: OncoRay - National Center for Radiation Research in Oncology, Medizinische Fakultät Carl Gustav Carus, TU Dresden, Fetscherstraße 74, PF 41, 01307 Dresden, Germany.
*E-mail address:* virginia.gambetta@oncoray.de (V. Gambetta).

[1] Shared first authorship.
[2] Shared senior authorship.
[3] Now with Med 360° Rheinland GmbH, Marie-Curie-Straße 12, 51377 Leverkusen.

https://doi.org/10.1016/j.phro.2025.100755
Received 8 October 2024; Received in revised form 10 March 2025; Accepted 17 March 2025
Available online 21 March 2025

## 1. Introduction

Intensity modulated proton therapy (IMPT) is affected by anatomical variations occurring during the treatment course [1–4], impacting proton range and overall treatment quality. Several *in vivo* treatment verification techniques have been proposed to monitor the compliance of the delivered dose distribution with the planned one. An online detected treatment deviation might serve as a trigger for stopping the current delivery and starting an adaptive workflow on demand. Timely response and online adaptation while the patient is on the treatment couch would be especially important for tumors in the thoracic, abdominal, or pelvic regions. These areas can exhibit considerable daily anatomical variations due to factors such as fluctuations in gastro-intestinal tract contents, bladder and rectum filling, breathing depth, or peritoneal fluid levels. In such cases, even fast offline adaptation would not be viable, as the anatomy might differ significantly at the next fraction [5]. An online-adaptive proton therapy (OAPT) workflow [6–9] triggered mid-delivery by treatment verification would aim to (1) assess dose deviations for the delivered first part of the scheduled plan and (2) adapt the remaining non-delivered part by considering and compensating the sub-optimally delivered dose up to the trigger point (background dose). In such verification-triggered OAPT workflow, it is essential to rely on an adaptive planning strategy that performs "partial" adaptation. A strategy for partial adaptation has already been investigated for head-and-neck cancer patients in the context of OAPT, with the goal of sparing in-room time during an online-adaptive workflow by performing parallel in-room and off-room tasks [10]. There, partial adaptation was applied to 3-field plans after the first field was delivered, with two remaining fields available for adaptation. Whether this type of triggered partial online adaptation can generate satisfactory fraction doses by compensating the suboptimal dose delivered before the intervention of a treatment verification system (e.g., by the first field) remains uncertain. This is especially challenging when only one treatment field is available for compensation, as for prostate cancer, typically treated with two-field plans.

Prompt-gamma based *in vivo* treatment verification (PGTV) offers both a safety net functionality, especially for standard OAPT based on pre-delivery in-room imaging, and the ability to detect anatomical changes during delivery [11–13], enabling a triggered OAPT workflow. The most advanced PGTV towards clinical translation is Prompt Gamma Imaging (PGI) [14–18], which maps the spatial distribution of prompt-gamma ray emission. At OncoRay, PGI is in clinical application in an observational study since 2015 and more than 450 clinical treatment fields have been monitored. Besides systematic assessment of PGI functionality [19–22], retrospective analysis of the real-world clinical data has proven its capability to detect anatomical changes in proton therapy treatments [23], in addition to verify proton range prediction in patients [24].

In this *in silico* study, we investigated the feasibility of partial adaptation to recover the total fraction dose distribution after the detection of relevant treatment deviations in the first field (i.e., after half of the plan delivery) for selected prostate cancer patients whose two-field proton therapy treatment was monitored by PGI. Ten fractions were selected where PGI analyses [23] had detected relevant treatment deviations, confirmed by the presence of anatomical changes in the corresponding in-room control computed tomography (cCT) scan. The conformity of the partially adapted fraction dose distributions was evaluated and compared to the initial, the fully re-optimized (assuming upfront imaging and plan adaptation at the beginning of each fraction) and the non-adapted dose distributions. A robustness evaluation was also performed.

## 2. Material and methods

### 2.1. Patient data

Treatment planning data and cCTs from ten fractions of eight prostate cancer patients were selected from a cohort treated at the University Proton Therapy Dresden (UPTD) within the PRompt-gamma-IMAging (PRIMA) study (PRIMA: DRKS00009224, ethics approval: EK181042015). In the PRIMA study, treatments are monitored regularly by PGI and an in-room cCT scan in treatment position was acquired for all monitored fractions. In the selected ten fractions, retrospectively analysed PGI data revealed relevant treatment deviations in at least one of the two horizontal opposing treatment fields, which were confirmed by anatomical variations in the cCT (Fig. 1). The field-wise PGI-based detection of relevant treatment deviations, as described in [23], served as the hypothetic trigger for the subsequent partial adaptation. This automatic field-wise identification of relevant or non-relevant treatment deviations applied the relative cumulative weight of spots with absolute range shifts $|r|$ above 5 mm ($W_{rel} = \frac{\sum_{i(|r_i|\geq 5mm)} w_i}{\sum_i w_i}$, where $i$ represents the number of spots in the field and $w_i$ their weights in terms of monitor units) as a binary classification parameter with a 6% threshold. The retrospectively identified anatomical variations included rectum filling changes (6x), femoral head offsets from leg rotations (6x) and subcutaneous tissue changes (10x) [23]. The retrospective use of cCTs from patients treated at UPTD for investigating online-adaptive planning strategies is approved by the local ethics committee (REACTION: BO-EK-347082023, PRIMA: EK181042015).

All planning CTs (pCTs) and in-room cCTs were acquired at SOMATOM Definition AS CT scanners (Siemens Healthineers, Forchheim) with the same dual-energy CT scan protocol (80/140 kVp) using single-source acquisition [25]. The cCTs were taken before the delivery, but assumed to be acquired after the delivery of the first field for which PGI detected the treatment deviation (Fig. 2A). Such first "delivered" field was chosen based on the PGI-detected deviations for each fraction, thus it does not necessarily correspond to the field actually delivered first. Considered regions-of-interest (ROIs) on the pCTs included a high-risk and a low-risk clinical target volume ($CTV_{High}$ and $CTV_{Low}$) and the organs-at-risk (OARs) bladder, rectum, penile bulb and femoral heads. The manual pCT-cCT registrations were reviewed by an experienced radiation therapist. OARs were recontoured on the cCTs for this study in RayStation v12.0.100 (RaySearch Laboratories AB, Stockholm) using deformable registration for penile bulb, femoral heads and seminal vesicles, and deep learning segmentation (RSL DLS Pelvic CT v.1.0.0) for prostate, bladder and rectum. Target contours were derived on the cCTs via margins and ROI algebra considering prostate, seminal vesicles, bladder and rectum contours, following the same approach as used for initial pCTs (Supplement 1). Final contours were reviewed and, if necessary, corrected by an experienced radiation oncologist.

The available clinical plans met the clinical goals according to in-house guidelines for prostate cancer treatments (Supplement 1, Table S1), considering a constant relative biological effectiveness (RBE) for protons of 1.1. The RBE-weighted doses are reported in Gy. The clinical robustly optimized IMPT plans delivered a simultaneous integrated boost of 60 Gy to $CTV_{High}$ and 48 Gy to $CTV_{Low}$ in 20 fractions with two opposing horizontal fields. Patient-specific range uncertainties of (2.7–4.3)%, corresponding to 2.0% uncertainty plus 2 mm [26], and setup uncertainties of (2.5–3.0) mm were considered for targets and selected OARs (rectum in all patients, bladder in half of the patients) in these "initial plans".

### 2.2. OAPT workflow triggered by online treatment verification

A PGI-triggered OAPT workflow was considered for the prostate cancer patients treated with 2-field plans (Fig. 2A). It was assumed that PGI detected the relevant treatment deviation during the delivery of the

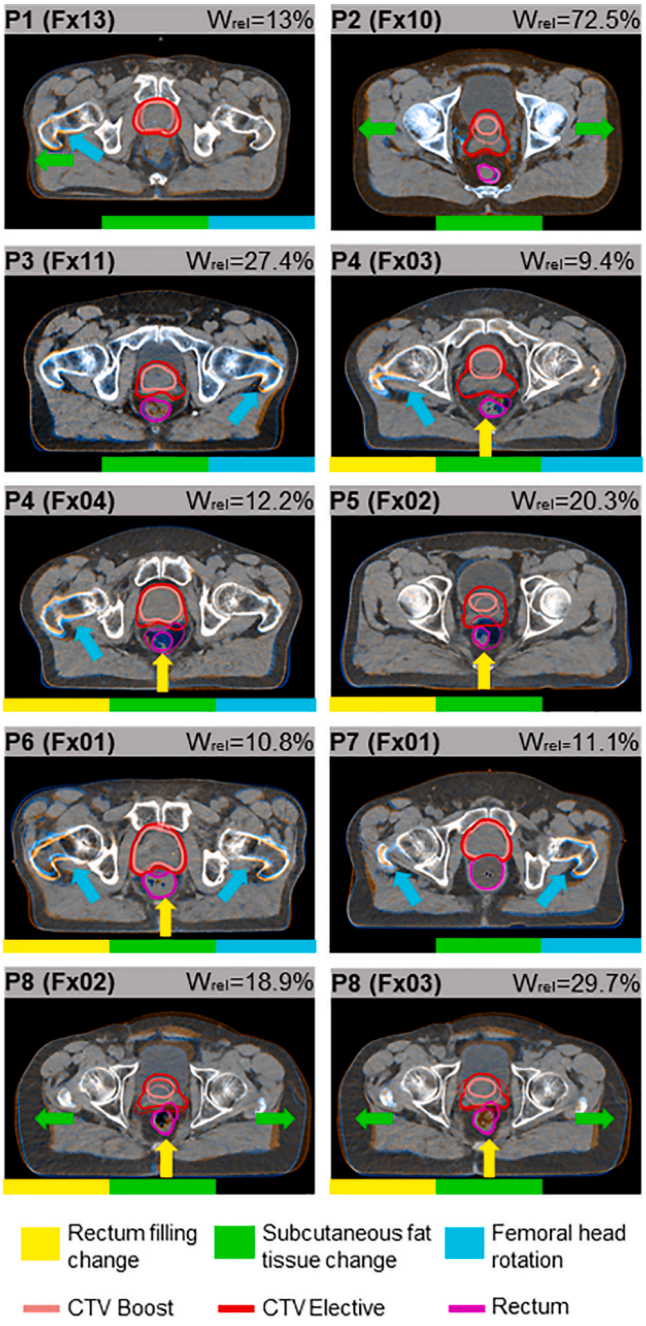


**Fig. 1.** Anatomical changes between planning (orange) and control CT (blue) visualized in a transversal slice for the ten selected treatment fractions (Fx) from eight patients (P1-P8). The overall identified anatomical changes were classified as rectum filling changes (yellow), femoral head rotations (cyan) and subcutaneous fat tissue changes (green), respectively. They are indicated by colored blocks at the bottom of each fusion image per fraction and, if visible in the presented slice, also by arrows in the respective color. Boost and elective clinical target volumes and the rectum are delineated in light pink, red and magenta, respectively. The value of the relative cumulative weight of spots with absolute range shifts $\geq$5 mm ($W_{rel}$) is also indicated for each investigated fraction.

first field, which would have triggered the stop of treatment after that field and the acquisition of a cCT. A partial plan adaptation of the remaining field was applied, considering the delivered first field dose distribution recalculated on the cCT as background dose. The objective was to demonstrate that partial adaptation can recover dose conformity for the whole fraction following the online detection of a treatment deviation.

### 2.3. Adaptive treatment planning

All cCT-based plans were generated in RayStation v12.0.100, with the clinical UPTD beam model and Monte Carlo dose engine v5.3 (0.3% uncertainty). Three delivery scenarios (Fig. 2B) were investigated: a non-adapted, a partially adapted and a fully adapted plan. To retrieve the non-adapted dose distributions, initial (clinical) plans were re-calculated on the cCTs. The optimal (fully adapted) fraction dose distributions were obtained by re-optimizing the initial plans on the cCTs while maintaining field angles, robustness settings and ROI-specific optimization objectives as in the initial plans. Partially adapted fraction doses were obtained via a script-based robust mimicking of a "reference dose", calculated as the fully adapted dose minus the background dose of the first non-adapted field. Such robust dose mimicking was performed via ROI-specific objective functions, known as "reference optimization" functions, which enforce a dose-volume-histogram-based or a voxel-wise mimicking of the dose in the respective ROI [10,27,28]. The resulting partial dose distribution was summed with the background dose to obtain the partially adapted fraction dose including both fields (non-adapted plus adapted). A timing evaluation of the proposed partial adaptation strategy with all subtasks is included in the Supplements (Supplement 2, Table S2).

### 2.4. Dosimetric analysis

The initial plans on the pCTs and the non–, fully and partially adapted ones on the cCTs were evaluated for target coverage and OAR sparing, according to the list of clinical goals. Selected dose-volume-histogram (DVH) parameters representing coverage of both $CTV_{High}$ and $CTV_{Low}$ ($D_{98\%}$>95%), hotspot dose of $CTV_{High}$ ($D_{2\%}$<107%), sparing of rectum ($V_{57Gy}$<5% as soft clinical goal and $V_{57Gy}$<10%), bladder ($V_{60Gy}$<3% as soft clinical goal and $V_{60Gy}$<5%) and penile bulb ($V_{49Gy}$<20% as soft clinical goal) were considered. An evaluation of additional DVH parameters for OAR sparing is available in Supplement 3 (Fig. S1 and Table S3).

A robustness evaluation of partially and fully adapted plans was performed for targets ($CTV_{High}$ and $CTV_{Low}$) and robustly optimized OARs (rectum and bladder). In total, 24 uncertainty scenarios were simulated per plan: eight setup shifts along the diagonal axes, combined with three density shifts, using the patient-specific robustness settings [29]. For each OAR, two different clinical goals (hard and soft) were evaluated. Results for worst-case scenarios were considered.

## 3. Results

### 3.1. Target coverage

In all ten fractions (Fig. 3A), partial and full adaptation led similarly to sufficient target coverages ($D_{98\%}$): the median results for $CTV_{Low}$/$CTV_{High}$ were 99.9%/98.0% for partial adaptation and 100.3%/98.7% for full adaptation. In contrast, non-adapted plans exhibited lower median values (98.7% and 94.5% for $CTV_{Low}$ and $CTV_{High}$, respectively) and failed the clinical goals for two ($CTV_{Low}$) and four ($CTV_{High}$) fractions. Median $D_{98\%}$ values for the initial plans were 99.4%/98.6% ($CTV_{Low}$/$CTV_{High}$). Hotspot dose $D_{2\%}$ to the $CTV_{High}$ was always below clinical goals with median values of 101.3%, 101.5%, 102.2% and 101.6% for the initial plan, no, partial and full adaptation, respectively.

### 3.2. OAR sparing

Dose values in OARs (Fig. 3B) were case-dependent for the initial plans, due to the different target vicinity to/overlap with OARs and patient characteristics. Dosimetric changes in rectum ($V_{57Gy}$) and penile bulb ($V_{49Gy}$) were similarly smaller for both partial and full adaptation

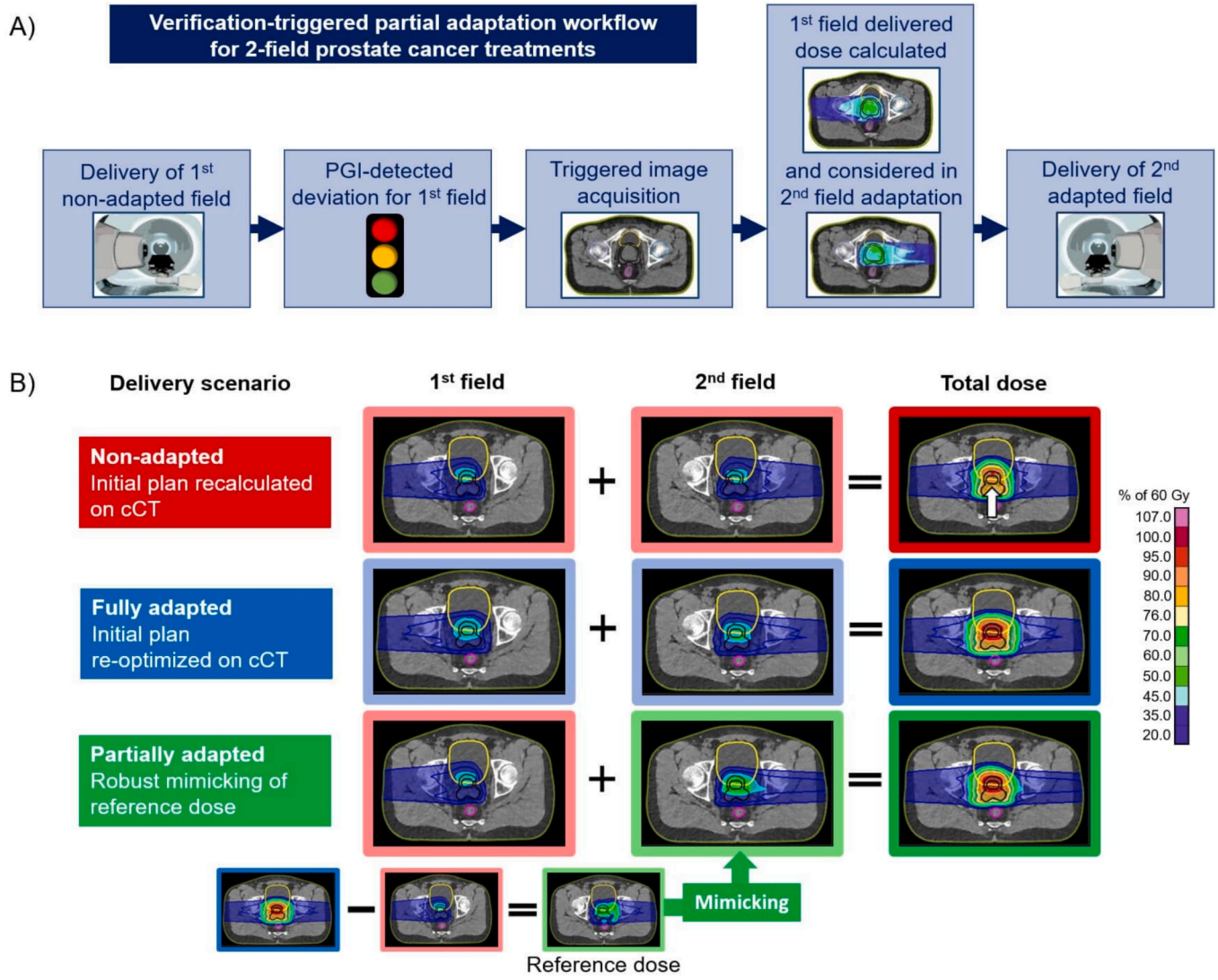


**Fig. 2.** A) Envisioned OAPT workflow for partial adaptation triggered by PGI, exemplary for a prostate cancer patient. B) Investigated delivery scenarios for one exemplary fraction: non-adapted, fully adapted and partially adapted (from top to bottom). For each scenario, the two fields (lighter outline) and the total dose distributions (darker outline) are shown, overlaid on the cCT for a selected slice. Clinical target volumes, rectum and bladder are delineated in black, fuchsia, and yellow, respectively. In this exemplary case, the non-adapted plan led to a drop in target coverage (white arrow), that was recovered by both the partially and fully adapted plans.

compared to no adaptation, which led more often to DVH-parameters above the clinical thresholds. For OARs closer to the CTVs, like the bladder, an increase in the investigated dosimetric parameter ($V_{60Gy}$) was observed for partial adaptation in comparison to other plans. However, all results were within the clinical goal.

### 3.3. Robustness evaluation

Generally, robustness was similarly preserved in all evaluated scenarios in most of the fractions for coverage of both targets and OAR sparing, with both adaptive strategies (Table 1). Full adaptation returned slightly superior results for the targets and the rectum soft constraint and comparable results for both the OARs hard goals in comparison with partial adaptation. Partial adaptation outperformed full adaptation for the bladder soft constraint.

## 4. Discussion

In this work, the planning strategy of partial adaptation was tested for the first time with clinical treatment plans and in the context of OAPT triggered by online treatment verification. Its feasibility in terms of achieving robust fraction dose distributions comparable to those from standard fully adapted plans has been proven for clinical two-field prostate cancer plans and treatment fractions, where PGI monitoring data from a clinical study indicated field-wise relevant treatment deviations. The strategy is a potential solution for future near real-time adaptations that may be triggered during the delivery by online treatment verification methods, and that may be applied only if necessary. This would benefit the treatment of entities highly susceptible to intrafractional variations and enhance the speed of overall OAPT workflows, improving patient comfort, decreasing costs and daily burden, and minimizing secondary cancer risks. Triggering online adaptation by verification could grant more flexible workflow options tailored to the specific situation, reduce the number of cCTs for certain cases, increase the safety and thereby potentially enable a further reduction of the uncertainty budget.

Current OAPT workflow developments mostly aim for an upfront adaptation performed before the start of daily fraction delivery [6,7,30,31], as exemplified by the first ever clinical OAPT implementation recently reported [32]. Integrating IMPT online treatment

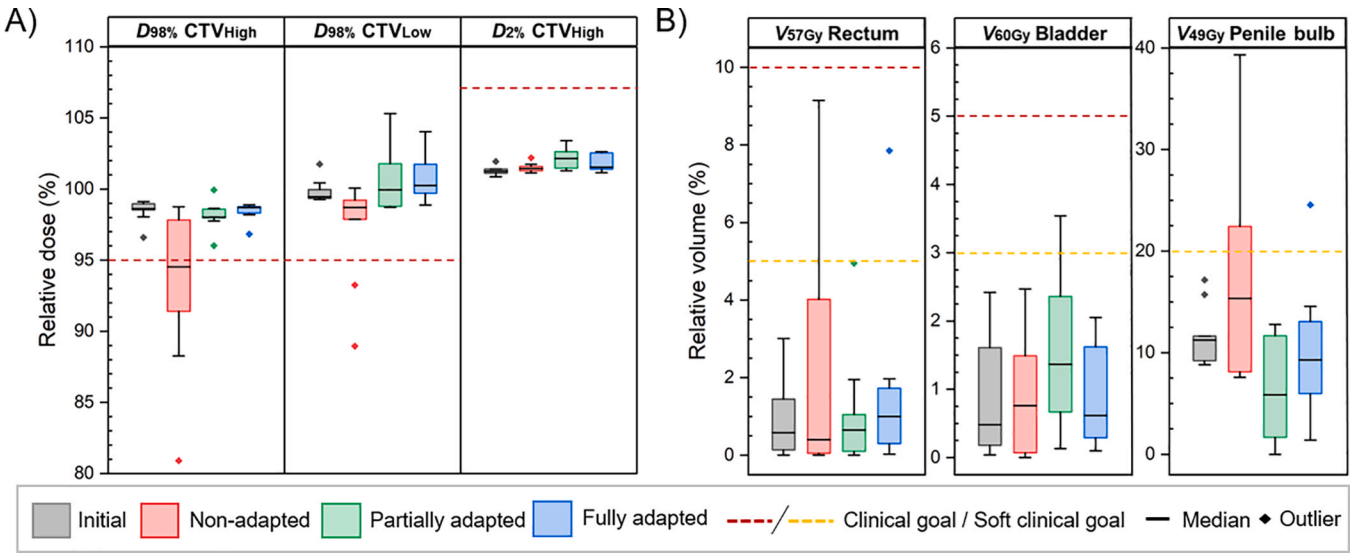


**Fig. 3.** Variation of DVH-parameters over the entire patient cohort for the four compared plans (initial and three adaptive strategies), representing CTV coverage and hotspots (A) and DVH-parameters to selected OARs (B).

**Table 1**
Number of plans (out of 10) passing the selected clinical goals for the investigated partial and full adaptations in the worst-case error scenario.

| Region of interest | Clinical goal | Number of adapted plans (out of 10) passing clinical goal in the worst-case perturbation scenario | |
|---|---|---|---|
| | | Partial adaptation | Full adaptation |
| $CTV_{High}$ | $D_{98\%} > 95\%$ | 7 | 9 |
| $CTV_{Low}$ | $D_{98\%} > 95\%$ | 8 | 10 |
| Rectum | $V_{57Gy} \leq 10\%$ (hard) | 10 | 10 |
| | $V_{57Gy} \leq 5\%$ (soft) | 9 | 10 |
| Bladder | $V_{60Gy} < 5\%$ (hard) | 8 | 9 |
| | $V_{60Gy} < 3\%$ (soft) | 7 | 6 |

verification would allow to detect treatment deviations mid-delivery, offering an additional opportunity for adapting not only before but also – or even exclusively – during treatment delivery. The information from the online treatment verification system would trigger the stop of the current treatment and the acquisition of a new image that is used for an appropriate plan adaptation. If a pre-delivery adaptation workflow were to be skipped, the online adaptation would then be "on demand" and triggered by treatment verification. Such a workflow including partial adaptation may only be deemed acceptable if the total delivered fraction dose is comparable to that of an upfront online adaptation.

We have previously introduced partial adaptation as a strategy to streamline upfront OAPT workflows for standardized 3-field IMPT plans of head-and-neck cancer patients in a proof-of-concept study [10]. There, we assumed that the first field delivery started after daily imaging while the adaption of the remaining two fields was ongoing. The partial adaptation of two fields compensated for the suboptimal background dose of the first non-adapted one. The study presented here investigated the performance of a partial online adaptation that could have been triggered by PGI after the first field delivery on 10 fractions (eight patients) of 2-field prostate cancer clinical plans. Having only one opposing field available for recovering dose conformity in the total fraction dose represents one of the most challenging settings for partial adaptation, especially for fractions with relevant treatment deviations in the background dose of the first field, as detected by PGI. Nevertheless, our findings imply that, with available online treatment verification, it would be possible to selectively initiate an online adaptation only for those fractions where deemed necessary. Instead of daily upfront imaging and subsequent evaluation of the adaptation need, one could directly start the daily treatment as scheduled, since effective adaptive workflows could be triggered later on if required. In this work, partial adaptation was considered to be triggered by PGI-detection of a relevant deviation, but in principle it would also work with other treatment verification techniques capable of online decision-making [33–37]. Moreover, partial adaptation was here assumed to be applied following the first field delivery, but could also be performed after the delivery of only a few energy layers [37].

The superior sparing of the partially adapted plans in comparison with non– and fully adapted ones for most investigated OARs aligned with previous findings [10]. A notable exception was the bladder, located very close to the target and even partially overlapping with it, where partial adaptation compromised OAR sparing to maintain target coverage robustness. However, all presented results ($V_{60Gy}$) for bladder sparing obtained with partial adaptation remained within the clinical goal, and for other DVH-parameters ($V_{50Gy}$, $V_{40Gy}$), a trend towards superior bladder sparing in comparison with no and full adaptation was revealed (Supplement 3, Fig. S1). Conversely, the results of the robustness evaluation for the rectum (Supplement 3, Table S3) favored full optimization.

The reference dose generation for the mimicking is still a limitation, relying on fully re-optimized plans, which would not necessarily be available in a realistic OAPT scenario. Potential alternatives, like the adoption of a predicted dose, are being investigated [38–40], as discussed in [10].

In a retrospective evaluation of clinically acquired PGI data, 44% (88/201) of monitored fields for prostate cancer treatments exhibited a relevant treatment deviation [23]. While this did not necessitate immediate adaptation during treatment, given the large safety margins in current clinical practice, it is a notable indicator of the potential application of OAPT, particularly in light of reduced margins. In the clinical study, the cCTs were acquired with the available in-room (fan-beam) CT scanner. This has relevant implications for the clinical applicability of the strategy, since the patient would be moved between fields in case any relevant deviations were detected, that triggered the acquisition of a new image. However, for future OAPT applications, the adoption of integrated imaging systems, like cone-beam CT, is highly anticipated and has the advantage to prevent unintended patient shifts as patient imaging takes place in treatment position at isocentre location. In terms of dealing with partial adaptation in a successive fraction, we expect either a full offline replanning in the case of gradual changes such as weight loss and external shrinkage, or possibly keeping the original plan

for the next fraction in case of random changes such as different rectal and bladder filling, or variations in positioning such as slight leg rotation with an effect on the femoral head in the beam path.

We disregarded intrafractional changes, assuming that the cCTs were representative of the anatomy after the first field delivery, even if they were originally acquired before the start of treatment. Intrafractional changes in prostate cancer depend mostly on variations of rectum and bladder fillings and on patient's movements and can have relevant dosimetric impact [41]. It has been reported that, during a radiotherapy fraction, the prostate can move more than 10 mm [42–44]. To minimize the effect of such variations, all patients included in the study had followed a drinking protocol before treatment and were treated with a balloon spacer (BioProtect Spacer; Tzur Yigal, Israel) located between prostate and rectum, with one patient (P7) receiving a water-filled endorectal balloon (Qfix, Avondale PA).

In conclusion, rapid intervention measures are critical to effectively address potential treatment deviations, like unanticipated inter-/intrafractional variations, and to streamline the online-adaptive process. OAPT triggered by treatment verification represents a promising approach, especially for entities (like prostate) highly prone to intrafractional variations. The presented retrospective evaluation of a PGI-triggered partial adaptation strategy is an important first step towards offering in-treatment adjustments through the development of near real-time OAPT triggered by treatment verification.

## Declaration of competing interest

The authors declare the following financial interests/personal relationships which may be considered as potential competing interests: OncoRay has a research collaboration with RaySearch Laboratories, IBA and PARTICLE on OAPT (ProtOnART consortium). OncoRay has an institutional research agreement with IBA. One of the co-authors is employed at RaySearch Laboratories (A.F.). For the present study, the authors received no external financial support neither for the study design or materials used, nor in the collection, analysis and interpretation of data, nor in the writing of the publication. The authors report no conflict of interest.

## Acknowledgments

The authors would like to thank Dr. Chirasak Khamfongkhruea, Julian Pietsch, Nick Piplack, Angelina Jost, and the OncoRay radiotherapy technologists' team led by Julia Thiele for the PGI acquisitions during clinical treatments within the PRIMA study and providing information about clinical treatments; and Prof. Dr. Steffen Löck for the helpful discussions and feedback about the obtained results.

## Appendix A. Supplementary data

Supplementary data to this article can be found online at https://doi.org/10.1016/j.phro.2025.100755.

## References

[1] Wang Y, Efstathiou JA, Sharp GC, Lu HM, Ciernik IF, Trofimov AV. Evaluation of the dosimetric impact of interfractional anatomical variations on prostate proton therapy using daily in-room CT images. Med Phys 2011;38(8):4623–33. https://doi.org/10.1118/1.3604152.

[2] Szeto YZ, Witte MG, van Kranen SR, Sonke JJ, Belderbos J, van Herk M. Effects of anatomical changes on pencil beam scanning proton plans in locally advanced NSCLC patients. Radiother Oncol 2016;120(2):286–92. https://doi.org/10.1016/j.radonc.2016.04.002.

[3] Stützer K, Jakobi A, Bandurska-Luque A, Barczyk S, Arnsmeyer C, Löck S, et al. Potential proton and photon dose degradation in advanced head and neck cancer patients by intratherapy changes. *J Appl Clin Med Phys* 2017;18(6):104–13. https://doi.org/10.1002/acm2.12189.

[4] Ashida R, Nakamura M, Yoshimura M, Mizowaki T. Impact of interfractional anatomical variation and setup correction methods on interfractional dose variation in IMPT and VMAT plans for pancreatic cancer patients: A planning study. *J Appl Clin Med Phys* 2020;21(7):49–59. https://doi.org/10.1002/acm2.12883.

[5] Zhang Y, Alshaiki J, Amos RA, Lowe M, Tan W, Bär E, et al. Improving workflow for adaptive proton therapy with predictive anatomical modelling: A proof of concept. Radiother Oncol 2022;173:93–101. https://doi.org/10.1016/j.radonc.2022.05.036.

[6] Albertini F, Matter M, Nenoff L, Zhang Y, Lomax A. Online daily adaptive proton therapy. Br J Radiol 2020;93:1107. https://doi.org/10.1259/bjr.20190594.

[7] Paganetti H, Botas P, Sharp GC, Winey B. Adaptive proton therapy. Phys Med Biol 2021;66(22):TR01. https://doi.org/10.1088/1361-6560/ac344f.

[8] Trnkova P, Zhang Y, Toshito T, Heijmen B, Richter C, Aznar MC, et al. A survey of practice patterns for adaptive particle therapy for interfractional changes. Phys Imaging Radiat Oncol 2023;26:100442. https://doi.org/10.1016/j.phro.2023.100442.

[9] Zhang Y, Trnkova P, Toshito T, Heijmen B, Richter C, Aznar M, et al. A survey of practice patterns for real-time intrafractional motion-management in particle therapy. *Phys Imaging Radiat Oncol* 2023;26:100439. https://doi.org/10.1016/j.phro.2023.100439.

[10] Gambetta V, Fredriksson A, Menkel S, Richter C, Stützer K. The partial adaptation strategy for online-adaptive proton therapy: A proof of concept study in head and neck cancer patients. *Med Phys* 2024;51(8):5572–81. https://doi.org/10.1002/mp.17178.

[11] Knopf AC, Lomax A. In vivo proton range verification: A review. Phys Med Biol 2013;58(15):131–60. https://doi.org/10.1088/0031-9155/58/15/R131.

[12] Parodi K, Polf JC. In vivo range verification in particle therapy. Med Phys 2018;45(11):e1036–50. https://doi.org/10.1002/mp.12960.

[13] Krimmer J, Dauvergne D, Létang J, Testa É. Prompt-gamma monitoring in hadrontherapy: A review. Nucl Instrum Methods Phys Res A 2018;878:58–73. https://doi.org/10.1016/j.nima.2017.07.063.

[14] Stichelbaut F, Jongen Y. Verification of the proton beam position in the patient by the detection of prompt gamma-rays emission. *39th meeting of the Particle Therapy Co-Operative Group (PTCOG)*. 2003.

[15] Smeets J, Roellinghoff F, Prieels D, Stichelbaut F, Benilov A, Busca P, et al. Prompt gamma imaging with a slit camera for real-time range control in proton therapy. Phys Med Biol 2018;57(11):3371–405. https://doi.org/10.1088/0031-9155/57/11/3371.

[16] Perali I, Celani A, Bombelli L, Fiorini C, Camera F, Clementel E, et al. Prompt gamma imaging of proton pencil beams at clinical dose rate. *Phys Med Biol* 2014;59(19):5849–71. https://doi.org/10.1088/0031-9155/59/19/5849.

[17] Richter C, Pausch G, Barczyk S, Priegnitz M, Keitz I, Thiele J, et al. First clinical application of a prompt gamma based in vivo proton range verification system. *Radiother Oncol* 2016;118(2):232–7. https://doi.org/10.1016/j.radonc.2016.01.004.

[18] Xie Y, Bentefour EH, Janssens G, Smeets J, Vander Stappen F, Hotoiu L, et al. Prompt Gamma Imaging for In Vivo Range Verification of Pencil Beam Scanning Proton Therapy. Int J Radiat Oncol Biol Phys 2017;99(1):210–28. https://doi.org/10.1016/j.ijrobp.2017.04.027.

[19] Priegnitz M, Barczyk S, Nenoff L, Golnik C, Keitz I, Wernet T, et al. Towards clinical application: prompt gamma imaging of passively scattered proton fields with a knife-edge slit camera. Phys med Biol 2016;61(22):7881–905. https://doi.org/10.1088/0031-9155/61/22/7881.

[20] Nenoff L, Priegnitz M, Janssens G, Petzoldt J, Wohlfahrt P, Trezza A, et al. Sensitivity of a prompt-gamma slit-camera to detect range shifts for proton treatment verification. Radiother Oncol 2017;125(3):534–40. https://doi.org/10.1016/j.radonc.2017.10.013.

[21] Khamfongkhruea C, Berthold J, Janssens G, Petzoldt J, Smeets J, Pausch G, et al. Classification of the source of treatment deviation in proton therapy using prompt-gamma imaging information. Med Phys 2020;47:5102–11. https://doi.org/10.1002/mp.14393.

[22] Pietsch J, Khamfongkhruea C, Berthold J, Janssens G, Stützer K, Löck S, et al. Automatic detection and classification of treatment deviations in proton therapy from realistically simulated prompt gamma imaging data. Med Phys 2023;50:506–17. https://doi.org/10.1002/mp.15975.

[23] Berthold J, Pietsch J, Piplack N, Khamfongkhruea C, Thiele J, Hölscher T, et al. Detectability of Anatomical Changes With Prompt-Gamma Imaging: First Systematic Evaluation of Clinical Application During Prostate-Cancer Proton Therapy. Int J Radiat Oncol Biol Phys 2023;117(3):718–29. https://doi.org/10.1016/j.ijrobp.2023.05.002.

[24] Berthold J, Khamfongkhruea C, Petzoldt J, Thiele J, Hölscher T, Wohlfahrt P, et al. First-In-Human Validation of CT-Based Proton Range Prediction Using Prompt Gamma Imaging in Prostate Cancer Treatments. Int J Radiat Oncol Biol Phys 2021;111(4):1033–43. https://doi.org/10.1016/j.ijrobp.2021.06.036.

[25] Wohlfahrt P, Möhler C, Hietschold V, Menkel S, Greilich S, Krause M, et al. Clinical Implementation of Dual-energy CT for Proton Treatment Planning on Pseudo-monoenergetic CT scans. *Int J Radiat Oncol Biol Phys* 2017;97(2):427–34. https://doi.org/10.1016/j.ijrobp.2016.10.022.

[26] Peters N, Wohlfahrt P, Hofmann C, Möhler C, Menkel S, Tschiche M, et al. Reduction of clinical safety margins in proton therapy enabled by the clinical implementation of dual-energy CT for direct stopping-power prediction. *Radiother Oncol* 2022;166:71–8. https://doi.org/10.1016/j.radonc.2021.11.002.

[27] Fredriksson A. Automated improvement of radiation therapy treatment plans by optimization under reference dose constraints. *Phys Med Biol* 2012;57(23):7799. https://doi.org/10.1088/0031-9155/57/23/7799.

[28] Kierkels RGJ, Fredriksson A, Both S, Langendijk JA, Scandurra D, Korevaar EW. Automated Robust Proton Planning Using Dose-Volume Histogram-Based Mimicking of the Photon Reference Dose and Reducing Organ at Risk Dose

Optimization. Int J Radiat Oncol Biol Phys 2019;103(1):251–8. https://doi.org/10.1016/j.ijrobp.2018.08.023.
[29] Korevaar EW, Habraken SJM, Scandurra D, Kierkels RGJ, Unipan M, Eenink MGC, et al. Practical robustness evaluation in radiotherapy – A photon and proton-proof alternative to PTV-based plan evaluation. Radiother Oncol 2019;141:267–74. https://doi.org/10.1016/j.radonc.2019.08.005.
[30] Nenoff L, Matter M, Charmillot M, Krier S, Uher K, Weber DC, et al. Experimental validation of daily adaptive proton therapy. Phys Med Biol 2021;66(20):5010. https://doi.org/10.1088/1361-6560/ac2b84.
[31] Stock M, Georg D, Ableitinger A, Zechner A, Utz A, Mumot M, et al. The technological basis for adaptive ion beam therapy at MedAustron : Status and outlook. *Z Med Phys* 2018;28(3):196–210. https://doi.org/10.1016/j.zemedi.2017.09.007.
[32] Albertini F, Czerska K, Vazquez M, Andaca I, Bachtiary B, Besson R, et al. First clinical implementation of a highly efficient daily online adapted proton therapy (DAPT) workflow. *Phys Med Biol* 2024;11(69). https://doi.org/10.1088/1361-6560/ad7cbd.
[33] Werner T, Berthold J, Hueso-González F, Koegler T, Petzoldt J, Roemer K, et al. Processing of prompt gamma-ray timing data for proton range measurements at a clinical beam delivery. Phys Med Biol 2019;64(10):105023. https://doi.org/10.1088/1361-6560/ab176d.
[34] Tattenberg S, Marants R, Niepel K, Bortfeld T, Sudhyadhom A, Landry G, et al. Validation of prompt gamma-ray spectroscopy for proton range verification in tissue-mimicking and porcine samples. *Phys Med Biol* 2022;67(20). https://doi.org/10.1088/1361-6560/ac950f.
[35] Huang Z, Tian L, Janssens G, Smeets J, Xie Y, Teo BK, et al. An experimental validation of a filtering approach for prompt gamma prediction in a research proton treatment planning system. Phys Med Biol 2024;69(15):155025. https://doi.org/10.1088/1361-6560/ad6116.
[36] Meijers A, Seller Oria C, Free J, Langendijk JA, Knopf AC, Both S. Technical Note: First report on an in vivo range probing quality control procedure for scanned proton beam therapy in head and neck cancer patients. Med Phys 2021;48(3):1372–80. https://doi.org/10.1002/mp.14713.
[37] Chen M, Yang D, Zhu XR, Ma L, Grosshans DR, Shao Y, et al. Investigation of intra-fractionated range guided adaptive proton therapy (RGAPT): (Part II) range-shift compensated on-line treatment adaptation and verification. Phys Med Biol 2024;69(15):5006. https://doi.org/10.1088/1361-6560/ad56f2.
[38] Borderias-Villarroel E, Fredriksson A, Cvilic S, Di Perri D, Longton E, Pierrard J, et al. Dose mimicking based strategies for online adaptive proton therapy of head and neck cancer. *Phys Med Biol* 2023;68(10):105002. https://doi.org/10.1088/1361-6560/accb38.
[39] Guerreiro F, Seravalli E, Janssens GO, Maduro JH, Knopf AC, Langendijk JA, et al. Deep learning prediction of proton and photon dose distributions for paediatric abdominal tumours. Radiother Oncol 2021;156:36–42. https://doi.org/10.1016/j.radonc.2020.11.026.
[40] Miyazaki K, Fujii Y, Yamada T, Kanehira T, Miyamoto N, Matsuura T, et al. Deformed dose restoration to account for tumor deformation and position changes for adaptive proton therapy. *Med Phys* 2023;50:675–87. https://doi.org/10.1002/mp.16149.
[41] Willoughby TR, Kupelian PA, Pouliot J, Shinohara S, Aubin M, Roach M, et al. Target localization and real-time tracking using the Calypso 4D localization system in patients with localized prostate cancer. Int J Radiat Oncol Biol Phys 2006;65(2):528–34. https://doi.org/10.1016/j.ijrobp.2006.01.050.
[42] Langen KM, Willoughby TR, Meeks SL, Santhanam A, Cunningham A, Levine L, et al. Observations on real-time prostate gland motion using electromagnetic tracking. Int J Radiat Oncol Biol Phys 2008;71(4):1084–90. https://doi.org/10.1016/j.ijrobp.2007.11.054.
[43] Nejad-Davarani SP, Sevak P, Moncion M, Garbarino K, Weiss S, Kim J, et al. Geometric and dosimetric impact of anatomical changes for MR-only radiation therapy for the prostate. J Appl Clin Med Phys 2019;20(4):10–7. https://doi.org/10.1002/acm2.12551.
[44] Ballhausen H, Li M, Hegemann NS, Ganswindt U, Belka C. Intra-fraction motion of the prostate is a random walk. Phys Med Biol 2015;60(2):549–63. https://doi.org/10.1088/0031-9155/60/2/549.